# 2.335-MeV Isobaric Analog Resonance in $^{51}V+p$ and the Excited States of $^{51}Cr$ Studied via the $(p, n)$ and $(p, n\gamma)$ Reactions*

J. J. Egan,† K. K. Sekharan, G. C. Dutt,‡ J. E. Wiest,§ and F. Gabbard
*Department of Physics and Astronomy, University of Kentucky, Lexington, Kentucky 40506*
(Received 27 December 1971)

The 2.335-MeV isobaric analog resonance in $^{51}V(p,n)^{51}Cr$ and $^{51}V(p,p)^{51}V$ was studied experimentally. Detailed analysis was not possible because of the complexity of the excitation function in this energy region. $^{51}V(p,n)^{51}Cr$ angular distributions at 4.013- and 5.016-MeV bombarding energies were analyzed via statistical-model formalism. 12 states in $^{51}Cr$ were observed up to an excitation energy of 2.39 MeV. The $\gamma$ rays from the transitions (777 → 749 keV) and (749 keV → ground state) have been observed and their angular distributions determined to be isotropic. Angular distributions of the 1165-, 1480-, and 2001-keV $\gamma$ rays leading to the ground state of $^{51}Cr$ have been measured at proton bombarding energies of 4.0 and 4.4 MeV. Spins of $\frac{9}{2}^-$ and $\frac{11}{2}^-$ are assigned to the 1165- and the 1480-keV levels, respectively, in agreement with other investigators. The angular distribution for the 2001-keV level is isotropic indicating a spin of $\frac{7}{2}$ or less. Higher excited states in $^{51}Cr$ were observed through the $(p,n)$ reaction at 2256, 2313, and 2380 keV. The $(p,n)$ yield coupled with the failure to observe the ground-state transition from the 2256-keV level in the $\gamma$-ray spectra indicates that the spin of this level is greater than $\frac{13}{2}$.

## I. INTRODUCTION

### A. 2.335-MeV Analog Resonance

A number of highly excited states in $^{52}Cr$ have been identified as the isobaric analogs of low-lying levels in $^{52}V$ by Teranishi and Furubayashi[1,2] from $(p,\gamma)$ and $(p,n)$ reactions on $^{51}V$ targets. 13 resonances in the compound nucleus were found below a proton bombarding energy of 2.6 MeV. The data in Refs. 1 and 2 are derived from high-resolution work done with thin targets. It shows much of the fine structure at the resonances. The strongest resonance in both the $(p,\gamma)$ and the $(p,n)$ work is the one seen at 2.335 MeV. Its parent state is the 1.557-MeV level in $^{52}V$. Teranishi and Furubayashi[2] fitted an average curve through the fine structure for this resonance in the $(p,n)$ data using the shape predicted by the theory due to Robson.[3,4] They measured only relative cross sections and obtained a fit by visually estimating a background level.

Shell-model calculations for $^{52}V$ by Vervier[5] with mixed configurations of $(\pi 1f_{7/2})^3$ with $(\nu 2p_{3/2})^1$, $(\nu 2p_{1/2})^1$, and $(\nu 1f_{5/2})^1$ have given a reasonably good representation of the low-lying states of $^{52}V$. This calculation indicates a $4^+$ level at 1.591 MeV with a spectroscopic factor for $l_n=1$ quite close to the experimental value for the 1.557-MeV level. It remains of some interest, then, to measure the cross sections through the various channels for this 2.335-MeV resonance.

In the present work the 2.335-MeV analog resonance has been investigated in the elastic scattering of protons from $^{51}V$ and in the reaction $^{51}V(p,n)^{51}Cr$. Absolute cross sections were obtained for both measurements. Attempts to fit the $(p,n)$ data were made by enhancing a transmission coefficient in the incident channel using the statistical-model formalism[6] according to the method described by Egan *et al.*[7] The $(p,n)$ data were taken with a 12-keV target, thick enough to average over the fine structure of the resonance.

The $^{51}V(p,p)^{51}V$ data were taken with a target with a thickness of 0.64 keV and the fine structure is quite apparent. It was necessary to use a thin target in order to see the effect of the resonance in the elastic scattering. At 2.3 MeV the Coulomb cross section is dominant, and the resonant effect is about 10% of the cross section at a laboratory angle of 163°.

### B. Excited States of $^{51}Cr$

There have been numerous studies of the levels in $^{51}Cr$. Early work utilizing the reaction $^{51}V(p,n\gamma)^{51}Cr$ has been done by Lobkowicz and Marmier and by Cassagnou *et al.*[8] Iyengar, Gupta, and Lal[9] have studied the neutron spectrum and the $\gamma$ rays produced in the reaction $^{51}V(p,n)^{51}Cr$. Comparison is made with statistical-model calculations in attempts to assign spins to states in $^{51}Cr$. Level positions up to an excitation energy of 7.931 MeV in $^{51}Cr$ have been reported by Robertshaw *et al.* and by Macgregor and Brown.[10] Robertshaw *et al.* have reported $l$ values for the transferred neutron, thereby assigning parity to many of the $^{51}Cr$ levels by measurements on the reaction $^{50}Cr$-

$(d,p)^{51}$Cr. More recent work leading to assignments of spins to levels up to an excitation energy of 4273 keV has been reported by Tepel, Malan, and deVillers[11] and by Sarantites and Winn.[12] The work of Tepel, Malan, and deVillers[11] yields spin assignments for the first six excited states of $^{51}$Cr through the study of $^{51}$V$(p,n)^{51}$Cr and $^{51}$V$(p,n\gamma)^{51}$Cr. Spin assignments are based on statistical-model[6] calculations of integrated $(p,n)$ cross sections and $\gamma$-ray angular distributions. Sarantites and Winn[12] have studied the reactions $^{51}$V$(p,n\gamma)^{51}$Cr and $^{48}$Ti-$(^4$He$,n\gamma)^{51}$Cr and have measured coincidences and angular correlations to ascertain branching ratios which are used with $(d,p)$ reaction studies to assign spins and parities to many levels. Comparison was made with model calculations.

Theoretical calculations for the levels in $^{51}$Cr have been made by McCullen, Bayman, and Zamick and Malik and Scholz.[13] Using a strong-coupling symmetric-rotator model, Malik and Scholz calculate energies of negative-parity levels with spins ranging from $\frac{1}{2}$ to $\frac{11}{2}$. McCullen *et al.* predict states with spins ranging from $\frac{1}{2}$ to $\frac{15}{2}$ using pure $1f_{7/2}$ configurations in a shell-model calculation.

The lifetimes of the 749- and 777-keV levels in $^{51}$Cr have been measured by Haar and Richter[14] who observed the cascade $\gamma$ ray with a proportional counter. Iyengar and Robertson[15] have also measured lifetimes of several excited states in $^{51}$Cr.

The present work was undertaken to obtain additional spectroscopic information about the excited states of $^{51}$Cr through the study of the $(p,n)$ and $(p,n\gamma)$ reactions. The neutron yields and angular distributions from the reaction $^{51}$V$(p,n)^{51}$Cr were measured employing the time-of-flight technique at proton bombarding energies of 4 and 5 MeV. The neutron angular distributions have not been previously reported and data have been obtained on higher excited states. Previous measurements were made at proton bombarding energies near 3 MeV. Our measurements were made at higher proton energy. New data have been obtained on the reaction $^{51}$V$(p,n\gamma)^{51}$Cr at proton bombarding energies of 2.7, 4.0, and 4.4 MeV. The data at 2.7 MeV were taken to measure the relative cross sections for the excitation of the 777- and 749-keV levels in $^{51}$Cr through the $(p,n)$ reaction. The angular distribution of the 28-keV cascade $\gamma$ ray (777 → 749 keV) was also measured. The $(p,n\gamma)$ measurement at 4.0 and 4.4 MeV gave new data on the 1165-, 1480-, and 2001-keV levels in $^{51}$Cr. Statistical-model analysis of the $(p,n)$ data[6,7] and the $(p,n\gamma)$ data[16] was performed to yield information about the spins and parities of the excited states in $^{51}$Cr.

## II. EXPERIMENTAL METHODS

### A. Elastic Scattering Measurements

Targets of $^{51}$V were made by vacuum evaporation of the natural vanadium metal onto carbon foils approximately 50 $\mu$g/cm$^2$ in thickness. A scattering chamber described previously by Scott[17] was used. The scattered protons were counted in three silicon surface-barrier detectors which were placed in the chamber at angles corresponding to zeros of Legendre polynomials. The three detectors were operated simultaneously, and a selective storage and signal-routing system facilitated the use of three separate memory blocks in a

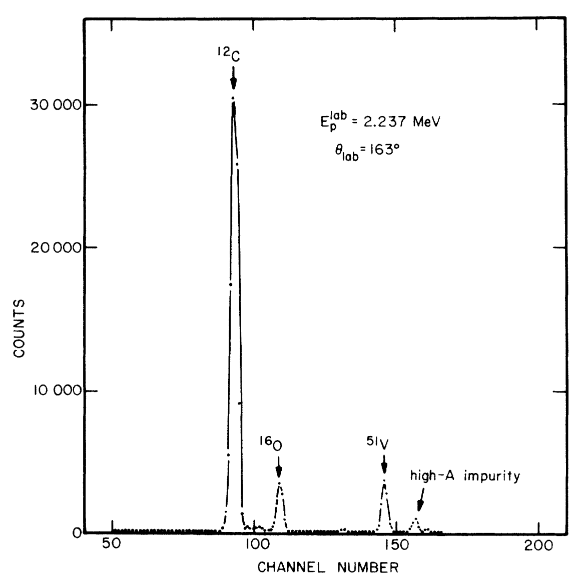


FIG. 1. A typical proton spectrum for protons scattered from $^{51}$V. Other peaks are from $^{12}$C in the foil, $^{16}$O, and a high-atomic-number impurity.

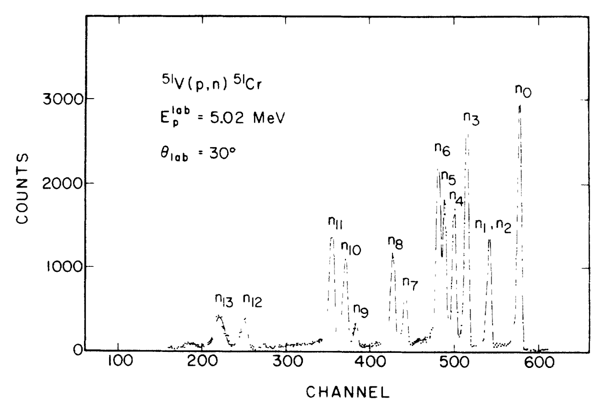


FIG. 2. A sample fit to a $^{51}$V$(p,n)^{51}$Cr spectrum using Tepel's data-reduction code.

4096-channel analyzer. Figure 1 is a typical proton spectrum from one of the surface-barrier detectors.

The target thickness was determined by Coulomb scattering within an error of ±5%. The yields from the proton peak were extracted by hand with an uncertainty of ±1.5%. The beam current was integrated to an estimated accuracy of ±2%, and the error in the measurement of the solid angle subtended by the detector was estimated to be ±1%. The errors combine to give an absolute uncertainty of ±6% on the differential cross sections and a relative uncertainty of ±1.5%.

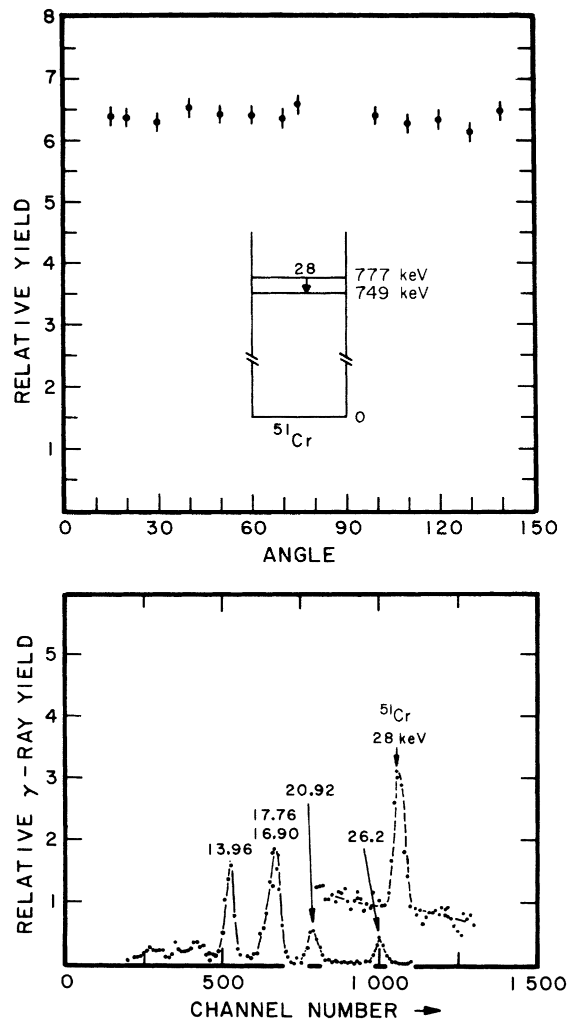


FIG. 3. Below: 28-keV $\gamma$-ray pulse-height spectrum for the incident proton energy $E_p = 2.7$ MeV, from the reaction $^{51}V(p, n\gamma)^{51}Cr$. Calibration lines from the $^{241}Am$ source are also shown. Above: The angular distribution for 28-keV $\gamma$ rays is shown. In the present experiment the energy of the $\gamma$ ray from the first excited level was found to be 749 ± 1.0 keV.

### B. $^{51}V(p,n)^{51}Cr$ and $^{51}V(p,n\gamma)^{51}Cr$ Measurements

The time-of-flight technique in conjunction with a pulsed proton beam was used in the detection of neutrons. Two detectors described previously[7] were used in this work.

For the data at 4 and 5 MeV, where the spectrum consists of many neutron groups, the terminal pulsed beam was bunched in a Mobley magnetic-bunching system. A computer code written by Tepel[18] was used to extract the yields from the spectra. Figure 2 is a typical time-of-flight spectrum. The lines in Fig. 2 represent a least-squares fit to the data. The code determines the background, fits isolated or overlapping peaks, and, in the output, gives the yield extracted from the peaks less the background, the error in the yield extraction, and a goodness-of-fit parameter.

The uncertainties in detection efficiency are the same as previously mentioned in Ref. 7. The uncertainties in the relative differential cross sections are 8–10%, and the standard errors in the absolute differential cross sections are estimated to be 15–20%. All error bars in the present work represent relative errors only.

The reaction $^{51}V(p,n\gamma)^{51}Cr$ was studied using a 5-mm-thick Ge(Li) detector to detect the 28-keV $\gamma$ rays and a 35-$cm^3$ Ge(Li) detector for the high-energy $\gamma$ rays. A 7-mg/$cm^2$-thick foil of natural vanadium (99.9% pure) was used as target. An aluminum chamber with a very thin wall (0.01 in.) was used as the target chamber to minimize absorption of 28-keV $\gamma$ rays in the chamber wall. The angular distribution of 28-keV $\gamma$ rays was measured at $E_p = 2.7$ MeV, whereas those of 1165-, 1480-, and 2001-keV $\gamma$ rays were measured at $E_p = 4.0$ and 4.4 MeV. The isotropic angular dis-

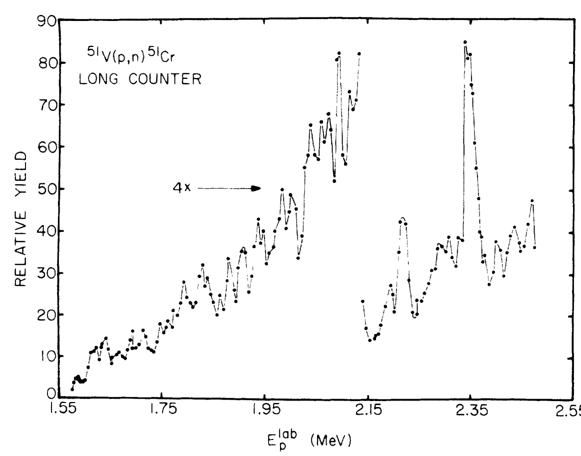


FIG. 4. Long-counter excitation function for the reaction $^{51}V(p,n)^{51}Cr$ up to the region of the 2.335-MeV analog resonance.

tribution of the 749-keV $\gamma$ ray was useful in checking the geometry of the experimental setup. The 28-keV pulse-height spectrum for the incident proton energy of $E_p = 2.7$ MeV, along with calibration lines from the $^{241}$Am source, is shown in Fig. 3 for the 5-mm detector.

The absolute efficiency of the 35-cm$^3$ Ge(Li) detector was measured using sources of $^{137}$Cs and $^{94}$Nb which emit $\gamma$ rays with energies of 662, 700, and 873 keV. The sources used were calibrated by the National Bureau of Standards. The relative efficiency of the 5-mm Ge(Li) detector was measured using the known intensity ratios of the radiations from an $^{241}$Am source. The x-ray and $\gamma$-ray radiation with energies of 13.9, 26.2, and 59.5 keV were employed. The absolute efficiency of the 5-mm detector was obtained by normalizing the relative data to 100% at 59.5 keV after correction for absorption in the Be entrance window.

## III. RESULTS AND ANALYSIS

### A. 2.335-MeV Analog Resonance

Figure 4 shows the relative neutron yield at 0° from the reaction $^{51}$V$(p,n)^{51}$Cr from a point just above the ground-state threshold[19] at 1.564 to 2.47 MeV. The threshold for the 749-keV first excited state is 2.328 MeV; hence, for the most part, Fig. 4 represents the yield of a single neutron group. The neutron yield in the region 2.312 to 2.47 MeV is dominated by the ground-state group, since the neutron yield to the 749-keV level in $^{51}$Cr, near the threshold for this level, is small compared with the yield of the ground-state with the yield of the ground-state group. The target used for these measurements was 15–20 keV thick. Even with the energy average provided by the thickness of the target much structure is apparent. The large anomaly at 2.335 MeV is the most prominent feature in the cross section.

Figure 5 shows proton elastic scattering data in the region of the 2.335-MeV isobaric analog resonance. The target was 0.64 keV thick for 2-MeV protons. Excitation functions were measured at the laboratory angles of 89, 124, and 163°. The first of these angles, in the center-of-mass system, is a zero of all odd-order Legendre polynomials; 124 and 140° are zeros of the $P_2$ and $P_3$ Legendre polynomials, respectively, in the center-of-mass system. 163° is the maximum angle at which it was possible to place a detector without interfering with the incident beam. Be-

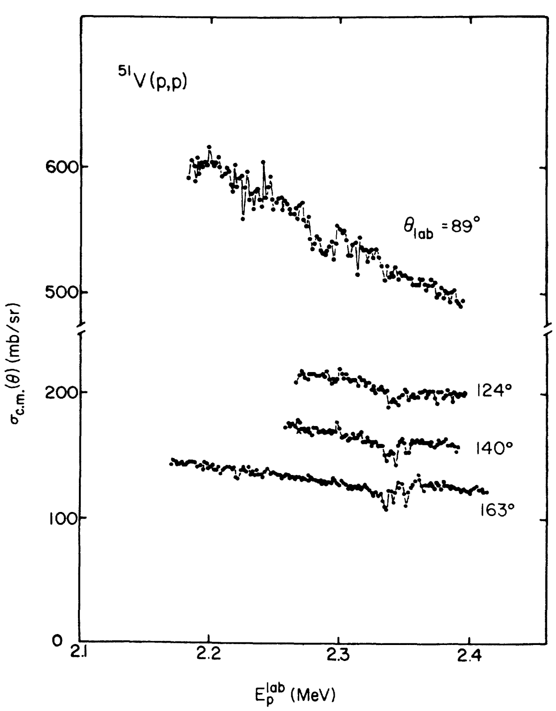


FIG. 5. $^{51}$V$(p,p)^{51}$V scattering cross section at several angles indicating an $l$ value of 1 for the 2.335-MeV analog resonance and considerable fine structure in the vicinity of the resonance.

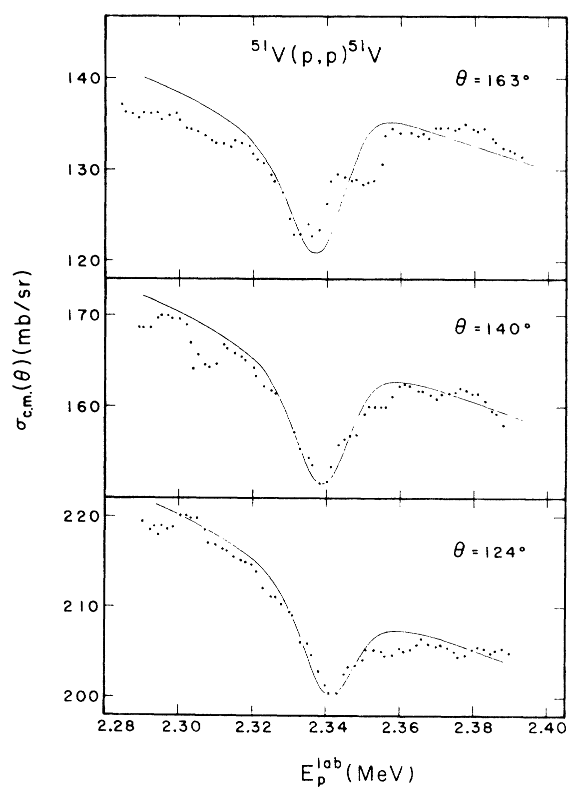


FIG. 6. Calculated fits to the elastic scattering excitation functions in the region of the 2.335-MeV analog resonance. Note that the zeros on the ordinate are suppressed.

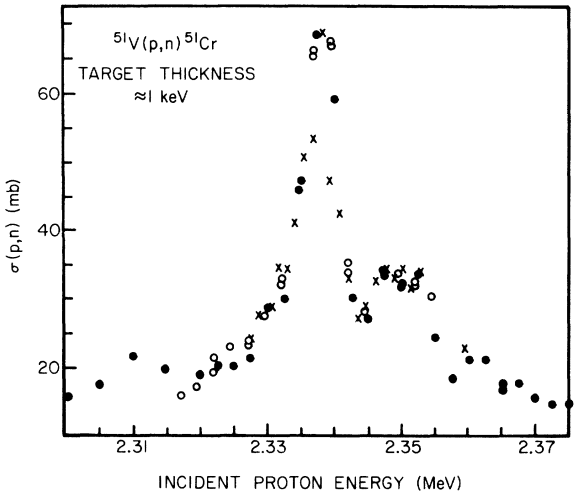


FIG. 7. The shape of the isobaric analog resonance at 2.335 MeV. The total neutron cross section was obtained by detecting the neutrons with a $4\pi$ neutron counter. Open circles, closed circles, and crosses are experimental values obtained by three repeated measurements. The resonance at about 2.335 MeV has a total width of 6 keV and the weak resonance at about 2.35 MeV has a width of 8 keV (Ref. 21).

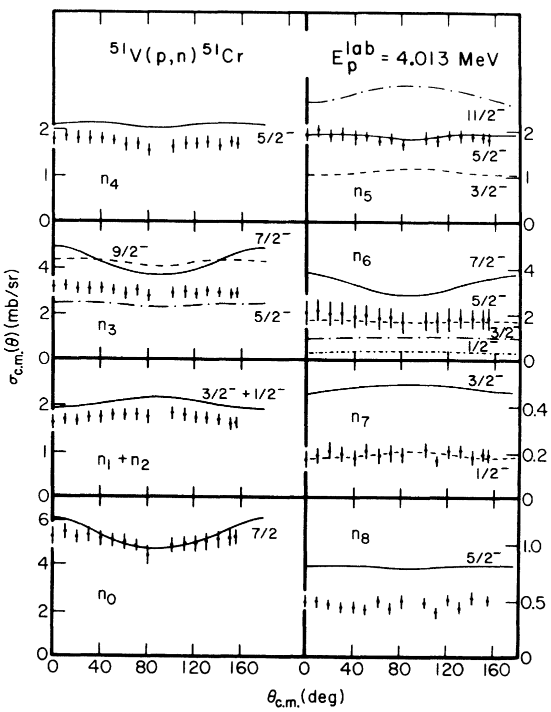


FIG. 8. Hauser-Feshbach fits to the 4.013-MeV angular distributions. Optical-model parameters are given in Table I and excitation energies corresponding to various neutron groups are given in Table III.

cause the Coulomb cross section is smallest at the most backward angle, the effect of the resonance is most pronounced in the 163° data. Since the resonance is not prominent in the 89° data, but is strong in the data at 124 and 140°, we conclude that protons which excite the resonance have orbital angular momentum $l_p = 1$.

Figure 6 shows a seven-point average of the elastic scattering data at 124, 140, and 163°. The zeros of the ordinates have been suppressed so that the resonance effect is more readily apparent. There is a rather strong suggestion in this averaged data that the resonance is a doublet.

Attempts were made to fit the elastic scattering data with a single resonance by a method similar to that of Scott *et al.*[20] The solid curve in Fig. 6 shows one such attempt. It seems clear that at least two resonances are contributing to this resonant effect. It is not possible to uniquely determine the spins of these resonances. Only the $l$ value for the incident protons at the large resonance is well determined by these data. The data are in-

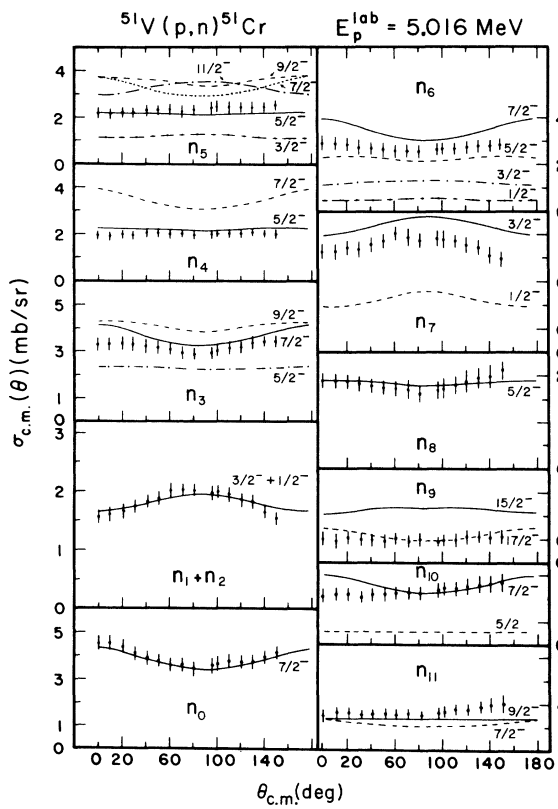


FIG. 9. Hauser-Feshbach fits to the 5.016-MeV angular distributions. Optical-model parameters are given in Table I. Computations were made with the computer program ALTE of Ref. 7. See Table III for identification of excited states corresponding to various neutron groups.

sufficient to determine, with certainty, the $l_p$ value of the smaller resonance. The variation of its differential cross section with angle indicates $l_p = 1$.

Sekharan and Mehta[21] have measured the total cross section for $^{51}V(p,n)^{51}Cr$ over a wide range of proton energy. Figure 7 shows their results near the 2.335-MeV resonance. These data show again that the structure is a doublet, with total experimental widths of about 6 and 8 keV, respectively.

Because of these uncertainties in the total spins and orbital angular momenta of these levels, we decided not to attempt more detailed analysis of the data near this resonance at the present time. Preliminary calculations show that the data can be explained by the superposition of two resonances with negative values of the parameter $\Delta$.[7,21]

The isobaric analog of the 2.335-MeV resonance in the compound system $^{52}Cr$ is the level in $^{52}V$ seen at 1.559 MeV in the $^{51}V(d,p)^{52}V$ work of Catala *et al.*[22] This level was also seen in a number of earlier investigations.[23-26] References 22 and 27 list this level as the ninth excited state in $^{52}V$. Van Aasche *et al.*[28] suggested $J^\pi$ of $4^+$ for this level on the basis of a comparison of the theoretical and experimental $B(M1)$ values for the decay of the state to a lower state at 846 keV seen via the reaction $^{51}V(n,\gamma)^{52}V$. Archer and Kennet[27] also deduced a $J^\pi$ of $4^+$ for this level. The $4^+$ assignment is in agreement with the choice of values $3^-$, $3^+$, or $4^+$ suggested by Carlos, Samama, and Andias[29] from an analysis of $\gamma$-$\gamma$ angular-correlation measurements on $^{52}V$ after thermal-neutron capture. A theoretical shell-model calculation by Vervier[5] predicts a $4^+$ level at 1.591 MeV which has an $l_n$ value of 1 and a calculated relative $(2J+1)S$ value of 103 relative to the ground-state value of $(2J+1)S = 100$ in the reaction $^{51}V(d,p)^{52}V$. The experimental value of $l_n$ for the 1.557-MeV level is 1 and the relative $(2J+1)S$ value[23] is 100. Hence, the value of $J^\pi$ was taken to be $4^+$ for the compound level in $^{52}Cr$ seen as a resonance at 2.335 MeV in the present work, and this value was used for the solid curves of Fig. 6.

### B. Excited States of $^{51}Cr$

The data for the excited states of $^{51}Cr$ consisted of neutron angular distributions for proton bombarding energies of 4.013 and 5.016 MeV shown in Figs. 8 and 9 and $\gamma$-ray angular distributions measured at proton energies of 2.7, 4.0, and 4.4 MeV. These $\gamma$-ray angular distributions are shown in Figs. 3 and 10.

The rather large statistical fluctuations which appear in the $^{51}V(p,n)^{51}Cr$ cross section make it necessary to average the yields over energy intervals of ~150 keV. The use of a target 150 keV thick would not permit the resolution of many of the neutron groups. Therefore, the data were taken with a target 30 keV thick and five different bombarding energies were used around 4 and 5 MeV. The 30-keV target permitted most of the excited states in $^{51}Cr$ to be resolved. In order to average over the fluctuations, the five angular distributions were added, point by point, to give $(p,n)$ angular distributions which are equivalent to those measured with a 150-keV target. This was done at 4.013 and 5.016 MeV. Data were obtained for 11 neutron groups. The curves in Figs. 8 and 9 represent statistical-model calculations[6,7] using transmission coefficients calculated with the optical-model potential whose parameters are listed in Table I. Calculations were performed for various spin assignments as shown in Figs. 8 and 9. In the case of the unresolved $n_1$ and $n_2$ neutron groups, the angular distributions shown represent the sum of these two groups.

The $^{51}V(p,n\gamma)^{51}Cr$ measurements shown in Figs.

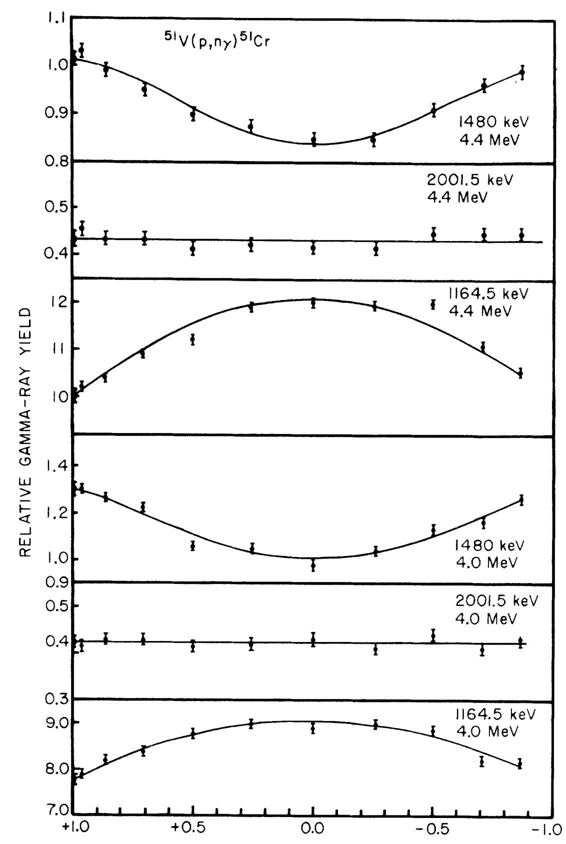


FIG. 10. Angular distributions of 1165-, 1480-, and 2001-keV $\gamma$ rays at $E_p = 4.0$ and 4.4 MeV. The solid lines are the least-squares fits to the experimental $\gamma$-ray yield.

TABLE I. Optical-model parameters used in the $^{51}V(p, n)^{51}Cr$ statistical-model calculations.

| | $V$ (MeV) | $r_V$ (F) | $a_V$ (F) | $W$ (MeV) | $r_W$ (F) | $a_W$ (F) | $V_{so}$ (MeV) |
|---|---|---|---|---|---|---|---|
| Protons | $59.5 - 0.5E$ | $1.25A^{1/3}$ | 0.65 | 4 | $1.25A^{1/3}$ | 0.47 | 7.5 |
| Neutrons | 47 | $1.30A^{1/3}$ | 0.62 | 5 [a] | $1.30A^{1/3}$ | 0.71 | 7.0 |

[a] The imaginary well for the neutrons is chosen to have a Gaussian form rather than a derivative Woods-Saxon form used for the protons (Ref. 7).

3 and 10 were made with a target whose thickness was 7 mg/cm$^2$. Data were obtained for proton bombarding energies of 2.7, 4.0, and 4.4 MeV. $\gamma$ rays with energies of 28 and 749 keV were observed at 2.7 MeV and $\gamma$ rays with energies of 1165, 1480, and 2001 keV were observed at energies of 4.0 and 4.4 MeV. The angular distribution shown in Fig. 3 is isotropic. The solid lines in Fig. 10 are least-squares fits of Legendre polynomials to the data. The coefficients for the polynomial fits are given in Table II.

The method employed in the analysis of the $\gamma$-ray data at 2.7 MeV was based on a calculation of the ratio of the intensity of the neutron groups $n_1$ and $n_2$ via the statistical model. The data for the 1165- and 1480-keV levels were analyzed using a method similar to that described by McEllistrem, Jones, and Sheppard.[16] A summary of spin-parity assignments for the levels studied in the present experiment is given in Table III.

### *749- and 777-keV Levels*

The $n_1$ and $n_2$ neutron groups exciting levels in $^{51}$Cr at 749 and 777 keV, respectively, were not resolved in the angular-distribution measurements of Figs. 8 and 9. These neutron groups were resolved at a proton energy of 3.5 MeV using a thin target and the spectrum is shown in Fig. 11. Stelson and co-workers[30] have also resolved these two neutron groups. Previously, there had been some question[11,31] as to whether the 777-keV level ($\frac{1}{2}^-$) was excited in the $(p, n)$ reaction.

In order to determine the relative intensity of the $n_1$ and $n_2$ neutron groups, the ratio of the number of 28-keV cascade $\gamma$ rays ($\frac{1}{2}^- \rightarrow \frac{3}{2}^-$) to the number of 749-keV $\gamma$ rays to the ground state ($\frac{3}{2}^- \rightarrow \frac{7}{2}^-$) was determined. Figure 3 shows a pulse-height spectrum for the 28-keV line along with calibration lines from $^{241}$Am. The energy of the $\gamma$ ray was determined to be $28.0 \pm 0.2$ keV. This $\gamma$ ray

TABLE II. Coefficients of the form $W(\theta) = 1 + A_2P_2(\cos\theta) + A_4P_4(\cos\theta)$ for the $\gamma$-ray angular distributions. Those in parentheses are theoretical calculations (Ref. 16) and those with uncertainties are from least-squares fits to the experimental values. $E_p$ = the bombarding proton energy, $E_\gamma$ = the $\gamma$-ray transition energy, and $\delta$ = the multipole mixing ratio of transitions.

| $E_\gamma$ (keV) | $J_x \rightarrow J_f$ | $E_p$ (MeV) | $A_2$ | $A_4$ | $\delta$ |
|---|---|---|---|---|---|
| 1165 | $\frac{9}{2}^- \rightarrow \frac{7}{2}^-$ | 4.0 | $-0.112 \pm 0.021$ ($-0.099$) | $-0.0031 \pm 0.0026$ ($-0.0054$) | $1.2 \pm 0.9$ |
| | $\frac{7}{2}^- \rightarrow \frac{7}{2}^-$ | 4.0 | $-0.0986$ (0.0184) | $-0.0039$ ($-0.0001$) | |
| | $\frac{5}{2}^- \rightarrow \frac{7}{2}^-$ | 4.0 | 0.1241 (0.010) | 0.0021 (0.0007) | |
| | $\frac{9}{2}^- \rightarrow \frac{7}{2}^-$ | 4.4 | $0.119 \pm 0.014$ (0.1257) | $-0.003 \pm 0.0022$ (0.0017) | $1.0 \pm 0.7$ |
| | $\frac{7}{2}^- \rightarrow \frac{7}{2}^-$ | 4.4 | $-0.1241$ ($-0.023$) | $-0.0021$ ($-0.004$) | |
| | $\frac{5}{2}^- \rightarrow \frac{7}{2}^-$ | 4.4 | $-0.1241$ ($-0.01$) | $-0.0021$ ($-0.0007$) | |
| 1480 | $\frac{11}{2}^- \rightarrow \frac{7}{2}^-$ | 4.0 | $0.1781 \pm 0.04$ (0.1749) | $0.0005 \pm 0.0017$ (0.0003) | $0.204 \pm 0.16$ |
| | $\frac{9}{2}^- \rightarrow \frac{7}{2}^-$ | 4.0 | 0.1897 (0.1118) | $-0.0232$ (0.0058) | |
| | $\frac{5}{2}^- \rightarrow \frac{7}{2}^-$ | 4.0 | 0.1897 (0.0281) | $-0.0232$ (0.0005) | |
| | $\frac{11}{2}^- \rightarrow \frac{7}{2}^-$ | 4.4 | $0.1207 \pm 0.043$ (0.1211) | $-0.0023 \pm 0.0022$ ($-0.0024$) | $0 \pm 0.132$ |
| | $\frac{9}{2}^- \rightarrow \frac{7}{2}^-$ | 4.4 | 0.1357 (0.1190) | $-0.0337$ ($-0.0031$) | |
| | $\frac{5}{2}^- \rightarrow \frac{7}{2}^-$ | 4.4 | 0.1357 (0.0227) | $-0.0337$ ($-0.0007$) | |

has been observed in other experiments.[14]

Figure 3 also shows the angular distribution of the 28-keV $\gamma$ ray along with a partial level scheme showing the transition measured. The isotropic distribution is consistent with the assignment of $\frac{1}{2}^-$ and $\frac{3}{2}^-$ to the 777- and 749-keV states, respectively.

The 749-keV $\gamma$ ray was observed with the 35-$cm^3$ Ge(Li) detector, and the ratio of the number of 749-keV $\gamma$ rays to 28-keV $\gamma$ rays was found to be $4.7 \pm 0.5$. This implies that the branching ratio, $B = \sigma(p,n)_{749}/\sigma(p,n)_{777}$ is $3.7 \pm 0.4$. Direct transitions from the 777-keV level to the ground state could not be observed because of interference from the 776-keV $\gamma$ ray between the 2256- and the 1480-keV levels.[12] The ratio of the intensity of the 777-keV $\gamma$ ray to the 749-keV $\gamma$ ray is estimated to be less than 1%. Earlier work[12,31] supports this conclusion.

A statistical-model calculation[6,7] was made using the optical-model parameters given in Table I. The weighted average branching ratio, $B$, was calculated to be 3.6 in good agreement with the experimental results and again supporting the assignment of $\frac{3}{2}^-$ and $\frac{1}{2}^-$ to these respective states.

### *1165-keV Level*

Sarantites and Winn[12] conclude from coincidence measurements of the 1165-keV $\gamma$ ray with $\gamma$ rays from other levels that a $\frac{9}{2}^-$ or $\frac{11}{2}^-$ assignment is favorable to this level, but $\frac{9}{2}^-$ is most probable. Tepel, Malan, and deVillers[11] measured angular distributions of this $\gamma$ ray at $E_p$ of 2832 and 3128 keV. From a comparison of the experimental anisotropy with theoretical predictions for different spin values they suggest $\frac{9}{2}^-$ or $\frac{5}{2}^-$ as the spin and parity for this level. From a comparison of the integrated $(p,n)$ cross section with Hauser-Feshbach calculations they rule out $\frac{5}{2}^-$.

In the present work, the shape of the angular distributions for the 1165-keV $\gamma$ ray at 4.0 and 4.4 MeV (Fig. 10) gives a unique assignment of $\frac{9}{2}^-$. In Fig. 12, $Q^2$ is shown as a function of arctan$\delta$, where $\delta$ is the mixing ratio, for three different spin values for this level. $Q^2$ is a minimum for $\frac{9}{2}$ at both proton energies. The corresponding values of $\delta$ are given in Table II.

The neutron angular distributions of Figs. 8 and 9 for $n_3$ agree with the shape of the calculated curve for $J^\pi = \frac{9}{2}^-$, but the magnitude of the cross section is consistently lower than the statistical-model calculation. The neutron data are consistent with the assignment of $\frac{9}{2}^-$. It should be emphasized that the shape of the angular distribution is a generally more reliable criterion for assigning spin than is the magnitude.[32] Unfortunately the shape of the angular distributions is not very sensitive to the value of the spin for the case of $^{51}V(p,n)^{51}Cr$.

TABLE III. Spin-parity assignments based on the present work compared with those of previous investigations.

| Neutron group | Excitation energy (keV) [a] | Previous $J^\pi$ assignments | $J^\pi$ [b] (Present work) |
|---|---|---|---|
| $n_0$ | 0 | $\frac{7}{2}^-$ | $\frac{7}{2}^-$ |
| $n_1$ | 749 | $\frac{3}{2}^-$ | $\frac{3}{2}^-$ |
| $n_2$ | 777 | $\frac{1}{2}^-$ | $\frac{1}{2}^-$ |
| $n_3$ | 1165 | $(\frac{9}{2}^-)$ | $\frac{9}{2}^-$ |
| $n_4$ | 1353 | $\frac{5}{2}^-$ | $\frac{5}{2}^-$ |
| $n_5$ | 1480 | $\frac{11}{2}^-$ | $\frac{11}{2}^-$ |
| $n_6$ | 1557 | $\frac{7}{2}^-$ | $(\frac{5}{2}^-, \frac{7}{2}^-)$ |
| $n_7$ | 1899 | $\frac{3}{2}^-$ | $(\frac{3}{2}^-)$ |
| $n_8$ | 2001 | $\frac{3}{2}^-, \frac{5}{2}^\pm, \frac{7}{2}^-$ | $(\frac{5}{2})$ |
| $n_9$ | 2256 | $\frac{9}{2}^+, \frac{11}{2}^\pm, \frac{13}{2}^\pm$ | $(\frac{15}{2}, \frac{17}{2})$ |
| $n_{10}$ | 2313 | $\frac{7}{2}^-$ | $\frac{7}{2}^-$ |
| $n_{11}$ | 2380 | $(\frac{7}{2}^-)$ | $(\frac{7}{2}, \frac{9}{2})$ |

[a] These are the excitation energies given by Ref. 12 rounded to the nearest keV.

[b] The parity is not determined by the statistical-model analysis of the $(p, n)$ data. This is taken from charged-particle data, mainly $(d, p)$ data of Ref. 10.

### *1480-keV Level*

Tepel, Malan, and deVillers[11] have measured the angular distribution of the 1480-keV $\gamma$ rays at $E_p = 3128$ keV and compared it with Hauser-Feshbach predictions. They assign $\frac{11}{2}^-$ to this level.

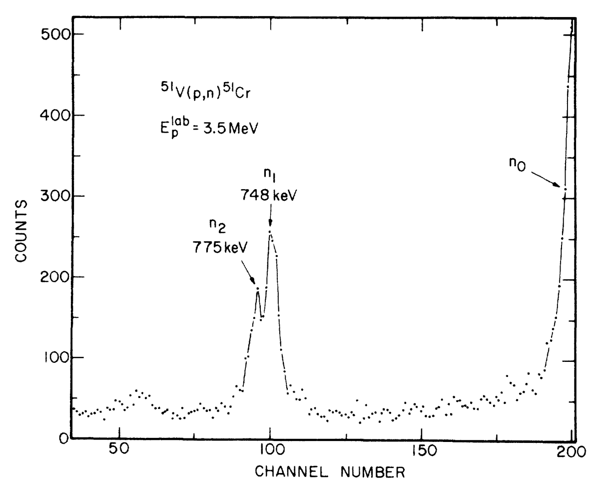


FIG. 11. A time-of-flight spectrum showing the resolved $n_1$ and $n_2$ neutron groups.

Our results from the $(p,n)$ measurements are not helpful for this level, because the neutron group, $n_5$, is not completely resolved from $n_6$. Analysis of the $\gamma$-ray angular distributions of Fig. 10 favors $J^\pi = \frac{11}{2}^-$ though it does not rule out $\frac{9}{2}^-$ according to the minimum $Q^2$ criterion for the angular distributions shown in Fig. 12. Other evidence[12] favors $\frac{11}{2}^-$ for this level.

### *1353- and 1557-keV Levels*

Sarantites and Winn[12] have discussed the assignment of $J^\pi$ to these levels. In Figs. 8 and 9 of the present work, the $(p,n)$ angular distributions are seen to strongly support the assignment of $J^\pi = \frac{5}{2}^-$ to the 1353-keV level. This neutron group, $n_4$, is well resolved and the shape of the angular distribution agrees well with this assignment while the shapes for other possible assignments, $J^\pi = \frac{7}{2}^-$ and $\frac{9}{2}^-$, do not fit the data. The $(p,n)$ data of Figs. 8 and 9 are not very helpful in the case of $n_6$, which corresponds to the 1557-keV level. $n_5$ and $n_6$ are not well resolved and the extraction of the yields is not very accurate. The assignment of $J^\pi = \frac{7}{2}^-$ is not inconsistent with the $(p,n)$ data, since the shape of the corresponding calculated curve agrees with the data.

### *1899-keV Level*

The 1899-keV level has been the subject of some controversy. Spins of $\frac{3}{2}^-$ and $\frac{1}{2}^-$ have been assigned. Robertshaw *et al.*[10] have pointed out that a $\frac{3}{2}^-$ assignment is a violation of the Lee-Schiffer[33] $J$-dependence rule. The $^{50}Cr(d,p)^{51}Cr$ value for $l_n$ is 1. The present work shows that $\frac{3}{2}^-$ gives the better fit to the data at 5.016 MeV and $\frac{1}{2}^-$ gives the better fit to the data at 4.013 MeV.

Sarantites and Winn[12] assign $\frac{3}{2}^-$ to this level on the basis of the strong decay to the ground state of $^{51}Cr$. Our $(p,n\gamma)$ work supports this conclusion, since a strong 1899-keV $\gamma$ ray was observed.

### *2001-keV Level*

The $(p,n)$ analysis of the 2001-keV data favors the assignment of $J=\frac{5}{2}$, but no $l_n$ value was determined from the $(d,p)$ work.[10] Our measurement of the $(p,n\gamma)$ shows the angular distribution to be isotropic indicating $J \le \frac{7}{2}$ for this level.

### *2256-keV Level*

No $\gamma$ ray resulting from direct decay of this level to the ground state was observed in the $(p,n\gamma)$ work. Sarantites and Winn[12] report decay to the 1480-keV level ($\frac{11}{2}^-$) indicating that the spin is greater than $\frac{11}{2}$.

The 2256-keV state is not strongly excited in the

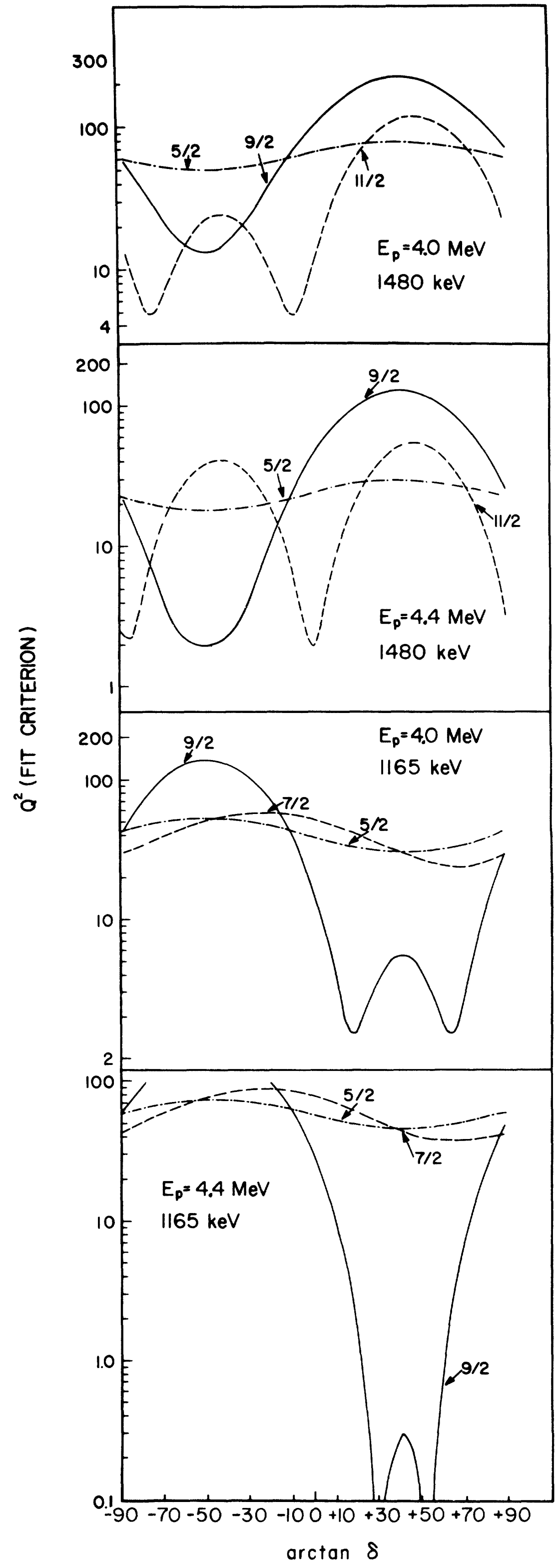


FIG. 12. Statistical criterion for the consistency with which the Hauser-Feshbach formula fits angular distributions.

$(p,n)$ reaction. The fact that such a level was not seen in any $(d,p)$[10] or $(n,\gamma)$ experiment[34] indicates that it is a high-spin state. States with spin-parity of $\frac{13}{2}^-$ and $\frac{15}{2}^-$ are predicted by the shell-model calculations of McCullen *et al.*[13] The best fit to the $(p,n)$ angular distribution of Fig. 9 was obtained by assuming a spin of $\frac{17}{2}^-$; however, a spin of $\frac{15}{2}$ gives a calculated cross section which is within a factor of 2 of the measured cross sections of Fig. 9. The only other spin value which gives a reasonable cross section is $\frac{1}{2}^{\pm}$, but no decay to the 749- and 777-keV levels is observed in the $(p,n\gamma)$ experiment. All other spin values from $\frac{3}{2}^{\pm}$ to $\frac{13}{2}^{\pm}$ give cross sections which are much too high to fit the data. Spins greater than $\frac{17}{2}$ give calculated cross sections which are much smaller than the data. Sarantites and Winn[12] rule out $J^\pi$ of $\frac{7}{2}^-$ or $\frac{9}{2}^-$ for this state on the basis of absence of decay to the ground state. A level has been tentatively identified by Stelson and Bass[35] in $^{51}V(p,n)^{51}Cr$ at approximately this energy, but no spin assignment was made. The evidence suggests $\frac{15}{2}$ or $\frac{17}{2}$ for this level.

### *2313- and 2380-keV Levels*

The 2313-keV state has been tentatively assigned $l_n=3$ in the $(d,p)$ work.[10] This yields possible values for $J^\pi$ of $\frac{5}{2}^-$ and $\frac{7}{2}^-$ and the present analysis favors $\frac{7}{2}^-$, although not convincingly, because of discrepancy in shape of the angular distribution. Several investigators[11, 12, 34] have assigned $\frac{7}{2}^-$ to this state and the $(p,n)$ data are consistent with this assignment.

The best fit to the $(p,n)$ data for the 2380-keV level was obtained assuming $J^\pi=\frac{7}{2}^-$ or $\frac{9}{2}^-$; however, the systematic errors in the data on this angular distribution are very large principally because of uncertainty in the detector efficiency for neutrons at this energy. Sarantites and Winn[12] indicated a level at 2386 keV with a high spin. Such a level would not be resolved from the 2380-keV level in the $(p,n)$ data of Fig. 9.

## IV. CONCLUSIONS

The results presented here illustrate the complexity of the isobaric analog states in $^{52}Cr$. Data previously interpreted as evidence for a positive level shift $\Delta$ for the 2.335-MeV resonance in $^{51}V+p$ are shown to be explained by the presence of a second resonance at 2.35 MeV. It is possible to represent the data by the superposition of two resonances with negative values of the parameter $\Delta$. Evidence that this parameter is always negative continues to accumulate.

The analysis of the $(p,n)$ and $(p,n\gamma)$ data presented confirm spin assignments in $^{51}Cr$ below an excitation energy of 1557 keV and yield information about spins of five additional levels up to an excitation energy of 2380 keV. The level at 2256 keV has a high spin, and it is suggested that this may be the state with a spin of $\frac{15}{2}$ expected on the basis of the shell-model calculations of McCullen *et al.*[13] All but one of the states predicted by assuming configurations of the type[4] $(\pi 1f_{7/2})^4(\nu 1f_{7/2})^{-1}$ and having an excitation energy less than 2.8 MeV have been observed. This model does not account for four of the levels observed in the experiments.

The Coriolis-coupling-model calculations of Malik and Scholz[13] can be made to reproduce the positions of the $\frac{3}{2}^-$ and $\frac{1}{2}^-$ levels near 0.78 MeV with a positive deformation of about 0.2. The model with this deformation qualitatively accounts for the levels observed in this experiment except that the high-spin state at 2256 keV is not predicted by the model.

## ACKNOWLEDGMENTS

The authors gratefully acknowledge the assistance of M. McPherson and D. E. Barnes in taking the data. Computer facilities were provided by the University of Kentucky Computing Center. Thanks are due the members of the staff of the machine shops and electronics shops for assistance in design and fabrication of the scattering chambers and detection equipment. We wish to thank Professor B. D. Kern and Professor M. T. McEllistrem for useful discussions. Professor McEllistrem also provided computer programs for analyzing the $\gamma$-ray angular distributions.

*Work supported in part by the National Science Foundation.

† Present address: Lowell Technological Institute, Lowell, Massachusetts.

‡ Present address: Trent University, Peterborough, Ontario, Canada.

§ Present address: Shawnee College, Ullin, Illinois 62992.

[1]E. Teranishi and B. Furubayashi, Phys. Letters 20, 511 (1966).

[2]E. Teranishi and B. Furubayashi, in *Isobaric Spin in Nuclear Physics*, edited by J. D. Fox and D. Robson (Academic, New York, 1966), p. 640.

[3]D. Robson, Phys. Rev. 137, B535 (1965).

[4]D. Robson, J. D. Fox, P. Richard, and C. F. Moore, Phys. Letters 18, 86 (1965); C. H. Johnson, R. L. Kernell, and S. Ramavataram, Nucl. Phys. A107, 21 (1968).

[5]J. Vervier, Nucl. Phys. 78, 497 (1966).

[6]L. Wolfenstein, Phys. Rev. 82, 690 (1951); W. Hauser and H. Feshbach, *ibid.* 87, 366 (1952); P. A. Moldauer, Rev. Mod. Phys. 36, 1079 (1964).
[7]J. J. Egan, G. C. Dutt, M. McPherson, and F. Gabbard, Phys. Rev. C 1, 1767 (1970). The computer program used for these computations was the program Alte [W. R. Smith, Oak Ridge National Laboratory Report No. ORNL-TM-1234 (unpublished); W. R. Smith, Comput. Phys. Commun. 1, 106, 181 (1970)].
[8]B. Lobhowicz and P. Marmier, Helv. Phys. Acta 34, 85 (1961); Y. Cassagnou, C. Levi, and L. Papineau, J. Phys. (Paris) 24, 881 (1963).
[9]K. V. K. Iyengar, S. K. Gupta, and B. Lal, Nucl. Phys. A96, 417 (1967).
[10]J. E. Robertshaw, S. Mecca, A. Sperduto, and W. W. Buechner, Phys. Rev. 170, 1013 (1968); A. Macgregor and G. Brown, Nucl. Phys. A88, 385 (1966).
[11]J. W. Tepel, J. G. Malan, and J. A. M. DeVillers, Nucl. Phys. A158, 129 (1970).
[12]D. G. Sarantites and W. G. Winn, Nucl. Phys. A155, 257 (1970).
[13]J. D. McCullen, B. F. Bayman, and L. Zamick, Phys. Rev. 134, B515 (1964); F. B. Malik and W. Scholz, *ibid.* 150, 919 (1966).
[14]M. C. Gregory and L. F. Hansen, Bull. Am. Phys. Soc. 16, 60 (1971); W. Haar and F. W. Richter, Z. Physik 231, 1 (1970).
[15]K. V. K. Iyengar and B. C. Robertson, Nuclear Research Centre, University of Alberta, Edmonton 7, Canada, Report No. 1 UAE NPL 1026 (unpublished).
[16]M. T. McEllistrem, K. W. Jones, and D. M. Sheppard, Phys. Rev. C 1, 1409 (1970).
[17]H. L. Scott, Ph.D. thesis, University of Kentucky, 1967 (unpublished).
[18]J. W. Tepel, Nucl. Instr. Methods 40, 100 (1966).
[19]C. H. Johnson, C. C. Trail, and A. Galonsky, Phys. Rev. 136, B1719 (1964).
[20]H. L. Scott, W. Galati, J. L. Weil, and M. T. McEllistrem, Phys. Rev. 172, 1139 (1968).
[21]K. K. Sekharan and M. K. Mehta, private communication.
[22]J. Catala, A. Garcia, J. M. Bolta, S. Hinds, H. Marchant, and A. E. Forest, Nucl. Phys. 74, 1 (1965).
[23]J. H. Bjerregaard, P. F. Dahl, O. Hamsen, and G. Sidenius, Nucl. Phys. 51, 641 (1964).
[24]J. E. Schwager and L. A. Cox, Phys. Rev. 92, 102 (1953).
[25]F. A. El Bedewi and S. Tadros, Nucl. Phys. 8, 71 (1958).
[26]A. W. Dalton, A. Kirk, G. Parry, and H. D. Scott, Proc. Phys. Soc. (London) 75, 95 (1960).
[27]N. P. Archer and T. J. Kennet, Can. J. Phys. 45, 2683 (1967).
[28]P. van Aasche, V. Gruber, B. P. Maier, H. R. Koch, O. W. B. Schult, and J. Vervier, Nucl. Phys. 79, 565 (1966).
[29]P. Carlos, R. Samama, and A. Andias, Nucl. Phys A93, 631 (1967).
[30]P. H. Stelson, private communication.
[31]K. V. K. Iyengar, B. Lal, S. K. Gupta, and M. D. Deshpande, Nucl. Phys. A93, 257 (1967).
[32]G. C. Dutt and F. Gabbard, Phys. Rev. 178, 1770 (1969).
[33]L. L. Lee and J. P. Schiffer, Phys. Rev. 154, 1097 (1967).
[34]G. A. Bartholomew, E. D. Earle, and M. R. Gunye, Can. J. Phys. 44, 2111 (1966); J. L. Alty, L. L. Green, G. D. Jones, and J. F. Sharpey-Schafer, Phys. Letters 13, 55 (1964).
[35]W. T. Bass, private communication.

PHYSICAL REVIEW C VOLUME 5, NUMBER 5 MAY 1972

# Proton-Nucleus Scattering and the Nuclear Forward-Scattering Amplitude*

Michael P. Keating and John G. Wills
*Department of Physics, Indiana University, Bloomington, Indiana 47401*
(Received 20 September 1971)

It is possible to extract the nuclear part of the forward-scattering amplitude from small-angle proton-nucleus elastic scattering. The process is complicated in practice by the effects of experimental errors and theoretical approximations. Optical-model calculations are done, using 14.5-MeV protons on $^{16}O$, $^{40}Ca$, and $^{90}Zr$, to examine the effects of these uncertainties on the determination of the nuclear forward amplitude.

## INTRODUCTION

The nuclear part of the forward-scattering amplitude is defined to be the exact amplitude minus the Coulomb amplitude. Holdeman and Thaler[1,2] have pointed out that this nuclear part of the amplitude becomes constant as the scattering angle approaches zero, while the Coulomb amplitude goes as $1/\sin^2\frac{1}{2}\theta$. Thus it is possible, in principle, to extract the real and imaginary parts of the nuclear forward amplitude from two elastic scattering measurements at small angles. If such amplitudes can be extracted from elastic scattering data, they would be useful in determining the reaction cross section, in putting restrictions on optical-model parameters, and in dispersion theory.

The obvious difficulty with this procedure is that